Inflammation-induced tumorigenesis in the colon is regulated by caspase-1 and NLRC4

Bo Hu[a,b,1], Eran Elinav[a,1], Samuel Huber[a], Carmen J. Booth[c], Till Strowig[a], Chengcheng Jin[a,d], Stephanie C. Eisenbarth[a,e], and Richard A. Flavell[a,f,2]

[a]Department of Immunobiology, [b]Department of Molecular Biophysics and Biochemistry, [c]Section of Comparative Medicine, [d]Department of Cell Biology, [e]Department of Laboratory Medicine, and [f]Howard Hughes Medical Institute, Yale University School of Medicine, New Haven, CT 06520

Contributed by Richard A. Flavell, November 9, 2010 (sent for review September 10, 2010)

Chronic inflammation is a known risk factor for tumorigenesis, yet the precise mechanism of this association is currently unknown. The inflammasome, a multiprotein complex formed by NOD-like receptor (NLR) family members, has recently been shown to orchestrate multiple innate and adaptive immune responses, yet its potential role in inflammation-induced cancer has been little studied. Using the azoxymethane and dextran sodium sulfate colitis-associated colorectal cancer model, we show that caspase-1–deficient (Casp1$^{-/-}$) mice have enhanced tumor formation. Surprisingly, the role of caspase-1 in tumorigenesis was not through regulation of colonic inflammation, but rather through regulation of colonic epithelial cell proliferation and apoptosis. Consequently, caspase-1–deficient mice demonstrate increased colonic epithelial cell proliferation in early stages of injury-induced tumor formation and reduced apoptosis in advanced tumors. We suggest a model in which the NLRC4 inflammasome is central to colonic inflammation-induced tumor formation through regulation of epithelial cell response to injury.

colon cancer | inflammation-induced colorectal cancer | NLR family, pyrin domain containing 3

Colorectal cancer is one of the most common forms of fatal cancer in the world, yet its underlying molecular pathogenesis is poorly understood (1). Chronic inflammation is a known risk factor for tumorigenesis, and epidemiological data suggest that up to 15% of human cancer incidence is associated with inflammation (2, 3). Inflammation-induced colorectal cancer develops in patients with chronic inflammatory bowel disease, with risk estimated to increase by 0.5 to 1% per year after 8 to 10 y of inflammatory bowel disease (4). The nature of this strong association is largely unknown, and suggested mechanisms include chronic formation of reactive oxygen species (5) and tumorigenesis induced by chronic epithelial exposure or inflammatory stimuli, such as IL-6 and TNF-α (6–9). The importance of inflammation is further highlighted by the dependence of tumor growth and progression on the activation of NF-κB by the classic inhibitor of nuclear factor kappa-B kinase-dependent pathway, which is crucial for tumor growth and progression (10).

Inflammasomes are multiprotein complexes formed by several members of the NOD-like receptor (NLR) family, procaspase-1, and the adaptor protein ASC, originally described by Tschopp and colleagues to be central mediators of the innate immune response (11). Certain NLR family members can mediate inflammasome assembly in response to diverse danger signals, including pathogen-derived factors, as well as molecules such as ATP, monosodium uric acid crystals, and aluminum hydroxide (11, 12). Upon activation, caspase-1 cleaves the proinflammatory cytokines IL-1β and IL-18, resulting in secretion of their mature forms (11). The NLRP3 (also known as CIAS1 and NALP3) inflammasome is the most thoroughly characterized inflammasome; it can be activated by a number of chemically and structurally diverse triggers (12–14) and has recently been shown to orchestrate multiple innate and adaptive immune responses (12, 15).

NLRC4 belongs to the NLR family with a characteristic N-terminal CARD domain, a central NACHT domain, and C-terminal leucine-rich repeats. The NLRC4 inflammasome has been demonstrated to be important in host defense against a number of Gram-negative bacterial pathogens, such as *Pseudomonas*, *Salmonella*, and *Shigella* (16–18). Specifically, the NLRC4 inflammasome is activated by flagellin and components of the Type III secretion system of pathogenic Gram-negative bacteria (18–20). Unlike other inflammasomes, NLRC4 can activate caspase-1 in an ASC-dependent or -independent manner (18, 21). Like other described inflammasomes, NLRC4 inflammasome formation results in secretion of IL-1β and IL-18, but can also induce caspase-1–mediated cell death (18, 22). Furthermore, NLRC4 has also been suggested to participate in apoptosis pathways downstream of p53, as NLRC4 gene expression induced by p53 contributes to p53-dependent apoptosis in several human cell types (23, 24).

In addition to orchestrating multiple innate and adaptive immune responses upon encountering pathogens, the NLRP3 inflammasome has also been demonstrated to take part in IL-1β–dependent adaptive immune responses against dying tumor cells (25). ATP released from chemotherapy-treated tumors activates the NLRP3 inflammasome in dendritic cells, resulting in an effective $CD8^+$ T-cell response directed against the tumor (25). However, the potential role of inflammasome signaling in the initiation and progression of inflammation-induced cancer has not been previously studied. Furthermore, mice deficient in MyD88, a central component in the signaling pathways downstream of the majority of Toll-like receptors (TLR), exhibit reduced tumor loads in a model of colon cancer (26). An explanation for this observation is that reduced colonic inflammation because of lack of TLR signaling following bacterial exposure decreases tumor formation in the colon. However, because MyD88 is also an essential component of the signaling cascade downstream of the IL-1 receptor family, the phenotype could be solely or partly explained by reduction of IL-1β and IL-18 signaling in the absence of a contribution of TLRs. We decided, therefore, to test this hypothesis in caspase-1–deficient mice that lack the ability to produce IL-1β and IL-18 and that should therefore have decreased inflammation-induced carcinogenesis. Support for the involvement of IL-18 came from a recent article in which IL-18$^{-/-}$ mice were shown to develop severe colitis and also increased tumorigenesis compared with WT, suggesting that enhanced tumorigenesis in TLR dysfunctional mice is linked to signaling through the IL-18 receptor (27). The role of inflammasome components in the pathogenesis of colonic autoinflammation remains controversial. Three recent reports suggested that deficiency in caspase-1, ASC, or NLRP3 in

Author contributions: B.H., E.E., S.C.E., and R.A.F. designed research; B.H., E.E., S.H., T.S., and C.J. performed research; C.J.B. contributed new reagents/analytic tools; B.H., E.E., S.H., C.J.B., T.S., C.J., and S.C.E. analyzed data; and B.H., E.E., S.C.E., and R.A.F. wrote the paper.

The authors declare no conflict of interest.

[1]B.H. and E.E. contributed equally to this work.

[2]To whom correspondence should be addressed. E-mail: richard.flavell@yale.edu.

This article contains supporting information online at www.pnas.org/lookup/suppl/doi:10.1073/pnas.1016814108/-/DCSupplemental.

mice was associated with an increased severity of chemically induced colitis and related tumorigenesis, suggested to be mediated in part by a defect in repair of the intestinal mucosa (28–30). However, opposite results were found in another study using the same chemically induced colitis model, demonstrating an ameliorated severity of colitis in NLRP3-deficient mice as a result of decreased levels of proinflammatory IL-1β (31). Differences between these studies may stem from methodological differences in the induction protocols as well as by inherent differences between variables, such as the composition of the intestinal flora.

In this article, we demonstrate a unique and surprising link between the inflammasome and colorectal inflammation-induced tumorigenesis. In contradiction to our hypothesis, we show that caspase-1–deficient mice have enhanced tumor formation in the azoxymethane (AOM) and dextran sodium sulfate (DSS) colitis-associated colorectal cancer (CAC) model. We demonstrate that the role of caspase-1 in tumorigenesis is mediated through direct and profound effects on colonic epithelial cell proliferation and apoptosis, rather than through regulation of colonic inflammation. Furthermore, we demonstrate that increased tumorigenesis is mediated through the NLRC4 inflammasome, rather than through NLRP3.

Results and Discussion

Caspase-1 Deficiency Enhances Inflammation-Induced Colorectal Tumor Formation. To study the effects of caspase 1 on inflammation-induced colorectal cancer, we used the AOM-DSS model, in which systemically administered AOM induces colon tumorigenesis in mice induced with chronic DSS colitis. In the AOM-DSS inflammation-induced colorectal tumor model (Fig. 1*A*), Casp1$^{-/-}$ mice featured a significant increase in tumor numbers and tumor load compared with WT mice (Fig. 1*B*). In advanced stages of disease (day 80), the heavy tumor load in 20% of Casp1$^{-/-}$ mice resulted in large bowel obstruction and prevented the passage of a murine endoscope (Fig. 1*C*). Histopathologically, tumors from Casp1$^{-/-}$ mice were indistinguishable from those of WT mice, where all tumors were composed of crypts and glands consistent with a well-differentiated adenocarcinoma (Fig. 1*D*, I). However, tumors of Casp1$^{-/-}$ mice appeared more aggressive with invasion (arrows) of tumor cells below the muscularis mucosae (*) noted in 75% of Casp1$^{-/-}$mice, compared with 14% invasion in WT group in advanced stages of disease (day 200) (Fig. 1*D*, II). No evidence of distal metastasis in the lungs, liver, spleen, or bone marrow was noted in mice that were killed on day 120 of the CAC regimen.

One potential mechanism contributing to the increased tumorigenesis in Casp1$^{-/-}$mice is increased colonic inflammation in these mice. To test this possibility, we used the acute DSS colitis model that employs a single 7-d-long cycle of DSS exposure (10). We did not observe any differences in mass loss (Fig. 2*A*), colonoscopic inflammation severity score (Fig. 2*B*), and histopathological morphology (Fig. 2 *C* and *D*), between Casp1$^{-/-}$ and WT mice at both early (6–8 d) and late stages of acute colitis (11–14 d), when substantial inflammation was notable both endoscopically and pathologically. Likewise, when chronic DSS colitis was induced by three 5-d cycles of DSS after AOM injection, no significant difference in chronic colonic inflammation were noted between Casp1$^{-/-}$ and WT mice (Fig. 2*E*). In addition, no significant changes were noted in both mRNA and protein levels of inflammatory cytokine in both acute and chronic DSS colitis (Fig. S1). This surprising result prompted us to investigate whether the dramatic enhancement in tumor formation observed in Casp1$^{-/-}$ mice may be caused by intrinsic effects in the colonic epithelial cells, rather than by indirect effects stemming from the degree of surrounding inflammation, as both hematopoietic and non-hematopoietic cells in the colon express caspase-1 (32). To investigate which of these cellular compartments is mainly responsible for the increased tumorigenesis in Casp1$^{-/-}$ mice, we created bone marrow-chimeric mice, which were induced with AOM-DSS inflammation-induced colon cancer. We found that both WT bone marrow transplanted Casp1$^{-/-}$ mice and Casp1$^{-/-}$ bone marrow transplanted WT mice did not recapitulate the

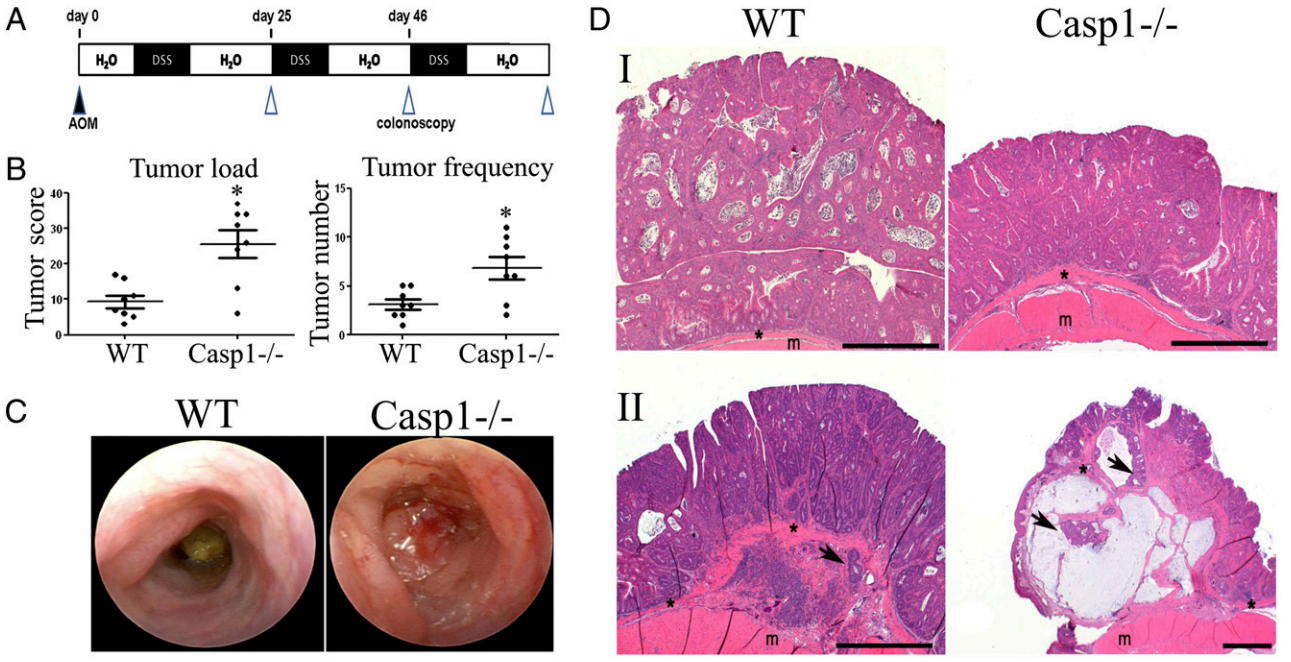

Fig. 1. Caspase-1 deficiency exacerbates AOM-DSS–induced colon cancer. (*A*) Schematic overview of the inflammation-induced cancer model. (*B*) Tumor load and tumor numbers/mouse in WT and caspase-1 KO (Casp1$^{-/-}$) mice (n = 8). P values < 0.05 were considered statistically significant. The experiments were repeated five times. (*C*) Representative colonoscopic appearance of WT and Casp1$^{-/-}$ mice colon on day 65 of AOM-DSS–induced color cancer. (*D*) Representative histopathologic sections of colon adenocarcinomas (*I*) and foci of tumor invasion (*II*) from WT and Casp1$^{-/-}$ mice. Invasive tumor foci (arrows) were smaller and less frequent in WT mice than Casp1$^{-/-}$ mice, where tumor foci were surrounded by abundant amounts of pale blue mucin. H&E staining; *muscularis mucosae; m, mascularis externa. (Scale bars, 200 μm.)

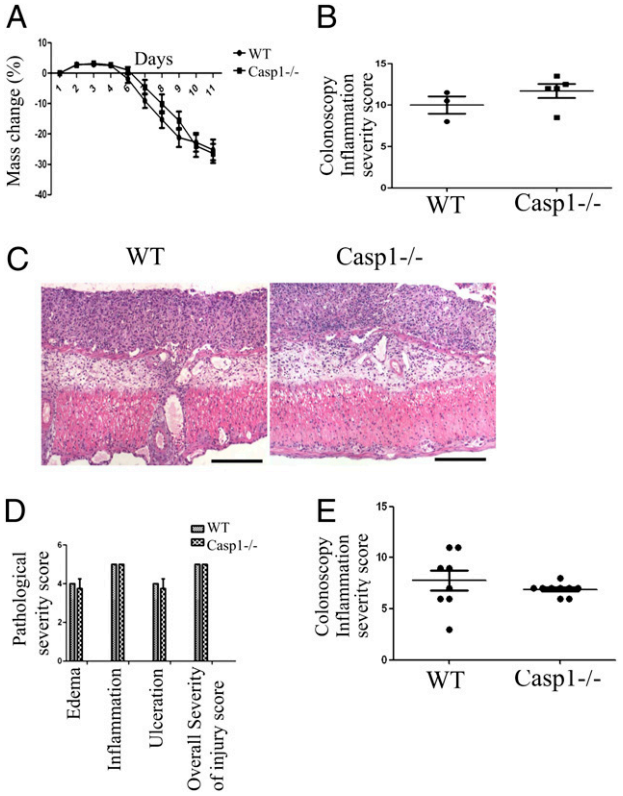

Fig. 2. No differences in inflammation between WT and Casp1$^{-/-}$ mice during acute DSS colitis. There were no significant difference in percent-mass change (*A*), colonoscopy inflammation severity score (*B*), severity of histopathological morphology (*C*) (H&E staining), or histopathology parameters for edema, inflammation, ulceration or overall severity of injury (*D*) between WT and Casp1$^{-/-}$ mice. (Scale bars in *C*, 200 μm.) (*E*) Likewise, the severity of chronic DSS colitis was similar between WT and Casp1$^{-/-}$ mice. All experiments were repeated twice.

Casp1$^{-/-}$ phenotype (Fig. S2). These data suggest that both the "radio-sensitive" hematopoietic compartment and the "radio-resistant" epithelial compartment are required for the increased tumorigenesis observed in Casp1$^{-/-}$ mice. However, involvement of prolonged antibiotic treatment in this model, which in our hands severely alters the microbiotic flora, results in increased variability between experiments and limits the interpretation of the bone-marrow transplantation results.

Enhanced Colon Epithelial and Tumor Cell Proliferation in Casp1$^{-/-}$ Mice During Inflammation-Induced Carcinogenesis. One of the suggested mechanisms to explain the initiation of colonic injury-induced cancer is repetitive epithelial cell destruction and subsequent regeneration, resulting in enhanced mutation (33, 34). To investigate this possibility, we analyzed the proliferation and survival of intestinal epithelial cells at day 15 of the CAC regimen in Casp1$^{-/-}$ and WT mice. At this stage, when inflammation is at its peak, the majority of the crypts appear normal in WT and Casp1$^{-/-}$ mice (Fig. 3*A*); however, small foci of crypt hyperplasia/dysplasia (Fig. 3*D*) were observed in both strains of mice. Immunohistochemistry with Ki67 (Fig. 3*B*) and BrdU (Fig. 3*C*), both markers of cellular proliferation, revealed significant increases in colon crypt cell proliferation in Casp1$^{-/-}$ mice compared with WT mice. However, in foci of crypt hyperplasia/dysplasia (Fig. 3*D*), there was no increase in the number of Ki67^{+} cells (Fig. 3*E*) and a moderate increase in the number of BrdU^{+} cells (Fig. 3*F*) in Casp1$^{-/-}$ mice when compared with WT mice. In advanced tumors at day 65 (Fig. 3*G*), the numbers of both Ki67^{+} cells (Fig. 3*H*) and BrdU^{+} cells (Fig. 3*I*) were higher in Casp1$^{-/-}$ mice compared with WT mice. Quantification of the immunohistochemical data validated the statistically significant increase in BrdU^{+} colonic epithelial cells in Casp1$^{-/-}$ mice at baseline, as well as an increase in Ki67^{+} and BrdU^{+} cells in both colonic and tumor tissue in advanced stages of the CAC regimen (Fig. S3). This validation suggests that a significantly increased proportion of cells in Casp1$^{-/-}$ tumors were actively proliferating compared with WT tumors. This difference may stem from caspase-1–dependent cleavage of a yet unrecognized negative regulator of cell proliferation. To further examine the possibility that epithelial cell survival and apoptosis also differ between Casp1$^{-/-}$ and WT mice, we performed in situ TUNEL staining on colon sections of mice in the early and late stages of AOM-DSS experiments. We noted no significant differences in TUNEL-positive cells in the colon between Casp1$^{-/-}$ and WT mice in the early stage of CAC (Fig. 3*J*, *Left*). In contrast, more advanced Casp1$^{-/-}$ tumors (day 65) exhibited a significantly reduced percentage of TUNEL-positive cells compared with WT mice (Fig. 3*J*, *Right*).

To address the question whether differences in antitumor immune responses contribute to the increased tumor formation in Casp1$^{-/-}$ mice, we stained colon sections from mice with advanced AOM-DSS–induced colon tumors (day 65 and day 200) with antibodies against CD3, Myeloperoxidase (MOP) and NK1.1. No differences were noted between the WT and KO mice in regard to infiltration of the tumor by T cells and neutrophils (CD3 staining: WT tumor: 47.20 ± 2.666 CD3^{+} cells/field; Casp1$^{-/-}$ tumor: 51.88 ± 3.193 CD3^{+} cells/field;MOP-1 staining: WT tumors: 18.50 ± 1.190 MOP-1^{+} cells/field, Casp1$^{-/-}$ tumors 19.42 ± 1.694 MOP-1^{+} cells/field; mice, $n \geq 6$, day 200 of the CAC regimen) and very rare NK1.1^{+} cells were noted in all samples, which is in agreement with the lack of difference in overall inflammation at earlier time points.

Increased Tumorigenesis in Casp1$^{-/-}$ Mice Is Mediated by the NLRC4 Inflammasome. Increased tumor formation in Casp1$^{-/-}$ mice suggests that inflammasome activation participates in pathways controlling the development and growth of tumors. The two most widely studied inflammasomes are the NLRP3 and NLRC4 inflammasomes. Both have been shown to participate in innate immune response to exogenous and endogenous "danger signals," such as ATP, crystals, and Gram-positive and -negative bacteria. In addition, the NLRC4 inflammasome has been suggested to participate in antiapoptosis pathways downstream of p53 (23, 24). To investigate the possible involvement of these NLRs in inflammation-induced cancer formation, we first examined the expression of caspase-1, NLRP3, and NLRC4 mRNAs in the epithelial and hematopoietic compartments of naive WT colons (Fig. 4*A*). Caspase-1 and NLRC4 were found to be relatively highly expressed in both colonic epithelial cells and CD45^{+} hematopoietic cells in the colon as compared with hypoxanthine phosphoribosyltransferase (HPRT). In contrast, NLRP3 expression was primarily restricted to the hematopoietic compartment. To evaluate their contribution to the increased tumor formation in Casp1$^{-/-}$ mice, we repeated the AOM-DSS inflammation-induced cancer model in NLRC4$^{-/-}$ and NLRP3$^{-/-}$ mice. No differences in tumor formation were observed between NLRP3$^{-/-}$ and WT mice (Fig. 4*B*). In contrast, NLRC4$^{-/-}$ mice had significantly increased tumor numbers and tumor load compared with WT mice (Fig. 4*C*). Similarly to Casp1$^{-/-}$ mice, tumors of NLRC4$^{-/-}$ mice appeared more aggressive with invasion (arrows) of tumor cells below the muscularis mucosae (*) noted in 66% of NLRC4$^{-/-}$ mice, compared with no invasion observed in WT group in advanced stages of disease (day 80) (Fig. S4). These results suggest that the differences in tumor formation noted in Casp1$^{-/-}$ mice are mediated through the NLRC4 inflammasome rather than the NLRP3 inflammasome. When DSS colitis was induced in NLRC4$^{-/-}$ mice, again no differences in inflammation severity were noted (Fig. 4 *D* and *E*, measuring mass loss or colonoscopy inflammation severity, respectively), further supporting the hypothesis that intrinsic,

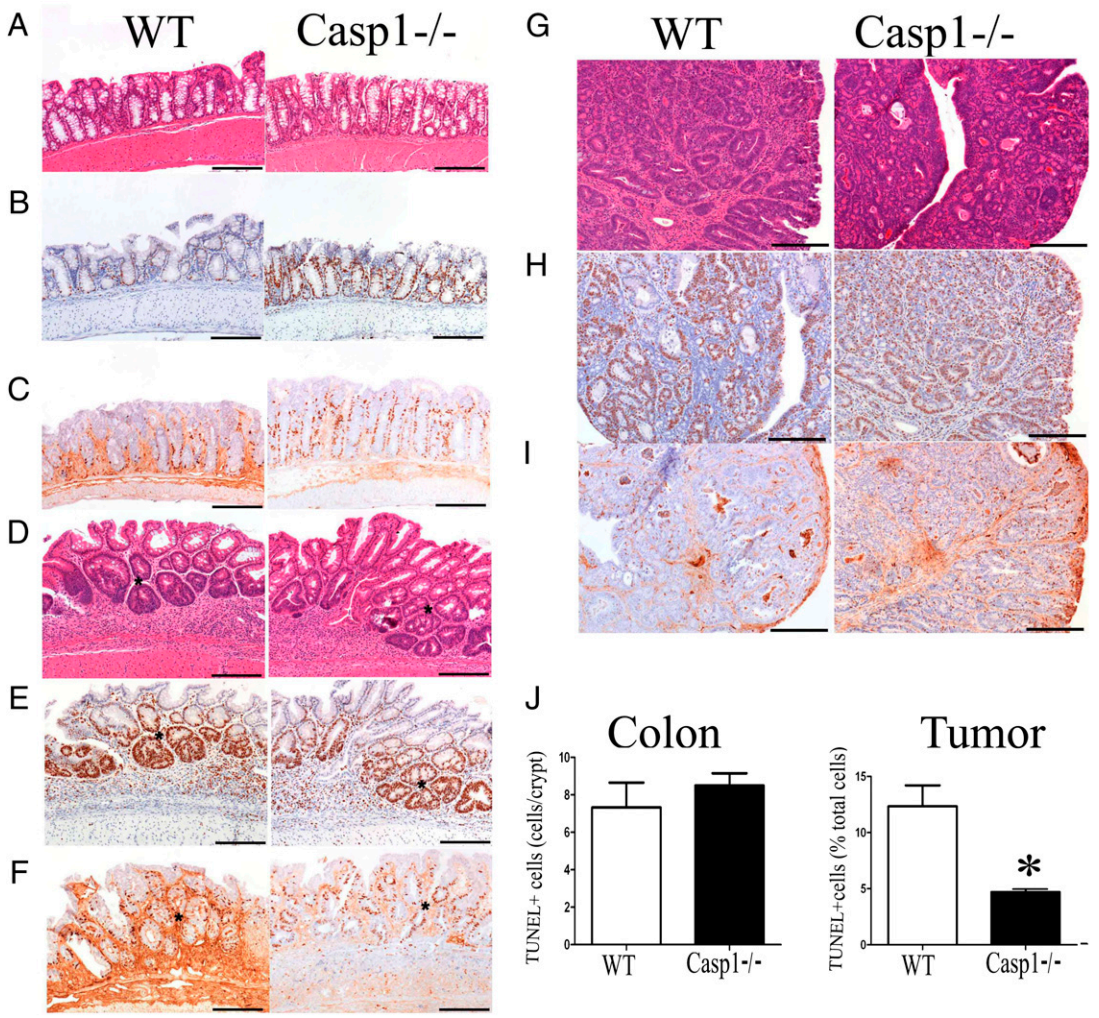

Fig. 3. Enhanced colon epithelial and tumor cell proliferation in Casp1$^{-/-}$ mice during inflammation-induced colorectal cancer. Representative H&E, Ki67, and BrdU immunohistochemistry at day 15 (*A–F*) and at day 65 (*G–I*), and TUNEL-positive cells in colons (day 8) and tumors (day 65) in WT and Casp1$^{-/-}$ mice given AOM-DSS. The majority of crypts at day 15 appeared normal (*A*); however, there were increased Ki67^{+} (*B*) and BrdU^{+} (*C*) crypt epithelial cells in Casp1$^{-/-}$ mice compared with WT mice. In foci of crypt hyperplasia/dysplasia (*D*), there were no significant difference in the number of Ki6^{+} cells (*E*) and a moderate increase in the number of BrdU^{+} cells (*F*) in Casp1$^{-/-}$compared with WT mice. At day 65 there were numerous large colon adenocarcinomas (*G*) with increased numbers of Ki67^{+} tumor cells (*H*) and BrdU^{+} tumor cells (*I*) in Casp1$^{-/-}$ compared with WT mice. (*A*, *D*, *G*: H&E staining; *B*, *C*, *E*, *F*, *H*, and *I*: DAB, Hematoxalyn) (Scale bars, 200 μm). (*J*) The number of TUNEL-positive cells in colon is similar in WT compared with Casp1$^{-/-}$ mice. In contrast, there is reduced cell death of tumor tissue in Casp1$^{-/-}$ mice (average cells counted: WT: 34.27 ± 8.964 positive cells/293.6 ± 86.39 total cells per field; Casp1$^{-/-}$: 16.87 ± 4.533 positive cells/364.2 ± 98.70 total cells per field). DNA fragmentation in WT and Casp-1$^{-/-}$ mice was determined on either whole-colon sections on day 8 of AOM-DSS model or tumor tissues at day 65. Error bars represent ± SEM, $P < 0.001$. The experiments were repeated two to three times.

rather than inflammation-related changes, account for the differences in tumor formation in inflammasome-deficient mice. As NLRC4 is implicated in p53-dependent apoptosis, it may provide a link to the increased tumorigenesis we observed in Casp1$^{-/-}$ mice and the changes in proliferation and apoptosis noted in epithelial cells in these mice (23). The fact that the NLRC4 inflammasome is activated by Gram-negative bacteria may point to its involvement in modulation of the colonic tumor formation by events involving the gut commensal bacterial flora (35). Future studies should aim to elucidate the patterns of molecular interaction between NLRC4 and caspase-1 that may lead to enhanced tumorigenesis in both. Our results differ from the report by Allen et al. which suggested that deficiency in NLRP3 but not in NLRC4 was associated with an increased severity of AOM-DSS–induced colorectal tumorigenesis (28). Difference between the studies may stem from methodological differences in the induction protocols as well as by inherent differences between variables, such as the composition of the intestinal flora.

To further study the molecular mechanism of Casp1$^{-/-}$ epithelial tumor transformation, we studied caspase-1 mRNA expression levels in normal colon tissue and colon tumors from WT mice. We observed a significant reduction in caspase-1 mRNA expression level in the tumor compared with colon tissue, suggesting that lack of caspase-1 may play a role in tumor progression (Fig. 4*F*). Furthermore, isolated colonic epithelial cells from either distal or proximal colons of mice with AOM-DSS–induced tumors featured a significant reduction in caspase-1 mRNA expression levels compared with naive mice, suggesting that reduction in caspase-1 expression specifically in epithelial cells may play a role in tumorigenesis (Fig. 4*G*). Similar results in humans showed that caspase-1 is down-regulated in human colon adenocarcinomas both at the mRNA and protein level (32). Similarly to Casp1$^{-/-}$ mice, NLRC4$^{-/-}$ mice featured significantly enhanced proliferation in both steady state and the early phase of inflammation-induced tumor formation and reduced apoptosis in tumors (Fig. S5).

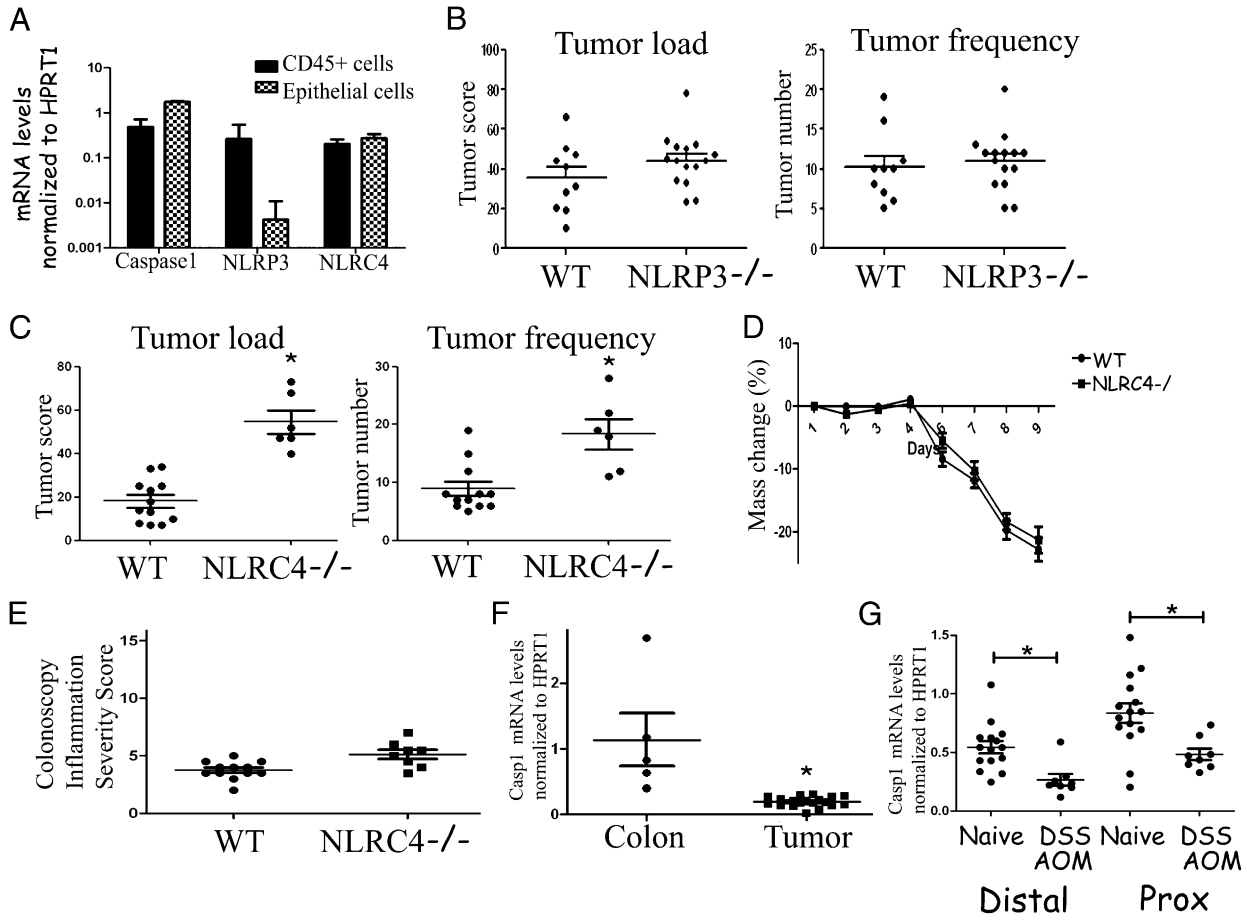

Fig. 4. Caspase-1–mediated tumor enhancement is mediated by the NLRC4 inflammasome. (*A*) Caspase-1, NLRP3, and NLRC4 mRNA expression in colon epithelial cells and CD45$^+$ cells. The levels of the indicated mRNAs were quantitated by real-time PCR and normalized to the level of HPRT mRNA. (*B*) Inflammation–induced tumor formation is similar in WT and NLRP3$^{-/-}$ mice ($n \geq 10$). The experiments were repeated three times. (*C*) NLRC4$^{-/-}$ mice feature enhanced inflammation-induced colon cancer compared with WT mice ($n \geq 6$); $P < 0.05$ was considered statistically significant. The experiments were repeated twice. Severity of DSS colitis in WT and NLRC4$^{-/-}$ mice, as evident by (*D*) mass change and (*E*) inflammation colonoscopy severity score. The experiments were repeated twice. (*F*) Caspase-1 mRNA expression in normal and colon and adjacent tumors from WT mice. mRNA levels were assessed by real-time PCR and normalized to the level of HPRT ($n \geq 5$). The experiment was repeated twice. $P < 0.05$ was considered statistically significant. (*G*) Caspase-1 mRNA expression in naive and AOM-DSS treated proximal and distal colonic epithelial cells from WT mice. mRNA levels were assessed by real-time PCR and normalized to the level of HPRT ($n \geq 8$). The experiment was repeated twice. $P < 0.05$ was considered statistically significant.

In conclusion, our results support a model in which caspase-1 is central in the prevention of colonic inflammation-induced tumor formation through regulation of the epithelial cell response to injury. These effects are mediated through the NLRC4 inflammasome. Lack of such activation results in intrinsic changes in epithelial gene-expression programming, including enhanced proliferation, reduced apoptosis in tumor tissue, and overall enhanced tendency for tumor formation. In agreement with our findings, inflammasome-deficient mice were recently suggested to feature enhanced tendency for inflammation-induced tumorigenesis, but in our studies we found no evidence for either enhanced DSS-induced inflammation in Casp1$^{-/-}$ mice, or major involvement of NLRP3 in contrast to the recent published reports (28, 29). Thus, our results rather support an intrinsic epithelial cell effect leading to enhanced tumorigenesis in the absence of caspase-1 or NLRC4 activity. Further deciphering of these mechanisms may enhance our understanding of events leading to inflammation-initiated tumor formation and may enable the recognition of new therapeutic targets.

Materials and Methods

Experimental Animals. All mice were cared for in accordance with institutional animal care and use committee-approved protocols at the Yale University School of Medicine animal facility.

Tumor Induction and Analysis. Age- and sex-matched cohoused 6- to 8-wk-old mice (WT, Casp1$^{-/-}$, NLRC4$^{-/-}$, and NLRP3$^{-/-}$ mice on C57BL/6 background) were injected with AOM (Sigma) intraperitoneally at a dose of 12.5 mg/kg body weight. After 5 d, mice were treated with 2.5% DSS (MP Biomedicals) (M.W. 36,000–50,000 Da) in the drinking water for 5 d, then followed by 16 d of regular water. This cycle was repeated twice (10).

DSS Colitis. To induce acute colitis, 6- to 8-wk-old mice (WT, Casp1$^{-/-}$, and NLRC4$^{-/-}$ mice on C57BL/6 background) were treated with 2% DSS (MP Biomedicals) (M.W., 36,000–50,000 Da) in the drinking water for 7 d followed by regular access to water. In the chronic colitis experiments, DSS was administered in three 5-d cycles, as is depicted in Fig. 1*A*.

Endoscopic Procedures. Colonoscopy was performed at indicated time points to monitor for severity of colitis and tumorigenesis according to murine endoscopic index of colitis severity system (36). A detailed endoscopic procedure is described in *SI Materials and Methods*.

Histopathology. After processing, colons were embedded lengthwise in paraffin (Blue RiBbon; Surgipath Medical Industries). Blocks were sectioned to the level of the lumen and then the next 5-μm section was stained with H&E, followed by placement of coverslips by routine methods. Colons were evaluated and were assigned scores by investigators blinded to experimental manipulation (37). A detailed histopathology procedure is described in *SI Materials and Methods*.

Isolation of Epithelial Cells and Hematopoietic Cells from the Intestine. Epithelial cells and hematopoietic cells were isolated from the freshly dissected colon by HBSS/EDTA shake and centrifugation. Detailed isolation procedures are described in *SI Materials and Methods*.

Immunohistochemistry. Paraffin-embedded sections were dehydrated and incubated with the following antibodies: anti-BrdU (1:4,000; Sigma), anti-Ki67 (1:100, Thermo; Lab Vision), anti-CD3 (1:400; Biocare Medical), anti-myeloperoxidase (1:100, Thermo; Lab Vision), anti-Nk1.1 (1:100, Novus Biologicals). DAKO EnVision System was used for detection. All sections were counterstained with hematoxylin. BrdU, TUNEL assay, and quantifications are detailed in *SI Materials and Methods*.

Colon Culture and ELISA. Sections of 1 cm of the proximal colon were cut, removed of feces, washed with PBS, and then cut half longitudinally. The colon sections were placed into culture in RPMI-1640 media (Sigma) with high concentration of penicillin and streptomycin and cultured at 37 °C with 5% CO_2. Supernatants were harvested after 24 or 36 h, and the concentration of cytokine was determined by ELISA. Antibody pairs were purchased from BD Pharmingen (IFN-γ) and SouthernBiotech (IL-17), and ELISA was performed according to the manufacturer's protocols.

RNA Analysis. Total RNA was extracted from colon tissue, tumors, and purified cells using TRIzol Reagent. SuperScript II Reverse Transcriptase (Invitrogen) was used for synthesis of cDNA. Real-time PCR analysis using TaqMan Fast Universal PCR Mater Mix and TaqMan Gene Expression Assays (Applied Biosystems) was performed on a 7500 Fast Real-time PCR system machine (Applied Biosystems). Expression data were normalized to HPRT. The primers are listed in *SI Materials and Methods*.

Statistical Analysis. Data are expressed as mean ± SEM. Differences were analyzed by Student's *t* test and one way ANOVA and post hoc analysis for multiple group comparison. P values < 0.05 were considered significant.

ACKNOWLEDGMENTS. We thank Lauren Zenewicz, Adam Williams, Tony Ferrandino, Jon Alderman, Elizabeth Eynon, Anthony Rongvaux, William O'Connor, Chozhavendan Rathinam, Yasushi Kobayashi, Jorge Henao Mejia, Paula Licona Limon, and all members of the R.A.F. laboratory; Namiko Hoshi for technical help and scientific discussion; Fran Manzo for manuscript preparation; Ruslan Medzhitov, David Schatz, and Patrick Sung for scientific discussion; and the Yale Research Histology Laboratory in the Department of Pathology and the Yale Mouse Research Histopathology in the Section of Comparative Medicine for histology and immunohistochemistry help. This study was funded in part by a Cancer Research Institute postdoctoral fellowship and by a supplemental grant by the United States-Israel Educational Foundation (to E.E.), Deutsche Forschungsgemeinschaft Hu1714/1-1 and the James Hudson Brown-Alexander Brown Postdoctoral Fellowships (to S.H.), National Institutes of Health Grant T32HI007974 (to S.C.E.), and the Howard Hughes Medical Institute (R.A.F.).

1. Weir HK, et al. (2003) Annual report to the nation on the status of cancer, 1975–2000, featuring the uses of surveillance data for cancer prevention and control. *J Natl Cancer Inst* 95:1276–1299.
2. Mantovani A, Allavena P, Sica A, Balkwill F (2008) Cancer-related inflammation. *Nature* 454:436–444.
3. Kuper H, Adami HO, Trichopoulos D (2000) Infections as a major preventable cause of human cancer. *J Intern Med* 248:171–183.
4. Askling J, et al. (2001) Family history as a risk factor for colorectal cancer in inflammatory bowel disease. *Gastroenterology* 120:1356–1362.
5. Coussens LM, Werb Z (2002) Inflammation and cancer. *Nature* 420:860–867.
6. Popivanova BK, et al. (2008) Blocking TNF-alpha in mice reduces colorectal carcinogenesis associated with chronic colitis. *J Clin Invest* 118:560–570.
7. Becker C, et al. (2004) TGF-beta suppresses tumor progression in colon cancer by inhibition of IL-6 trans-signaling. *Immunity* 21:491–501.
8. Bollrath J, et al. (2009) gp130-mediated Stat3 activation in enterocytes regulates cell survival and cell-cycle progression during colitis-associated tumorigenesis. *Cancer Cell* 15:91–102.
9. Grivennikov S, et al. (2009) IL-6 and Stat3 are required for survival of intestinal epithelial cells and development of colitis-associated cancer. *Cancer Cell* 15:103–113.
10. Greten FR, et al. (2004) IKKbeta links inflammation and tumorigenesis in a mouse model of colitis-associated cancer. *Cell* 118:285–296.
11. Martinon F, Burns K, Tschopp J (2002) The inflammasome: A molecular platform triggering activation of inflammatory caspases and processing of proIL-beta. *Mol Cell* 10:417–426.
12. Eisenbarth SC, Colegio OR, O'Connor W, Sutterwala FS, Flavell RA (2008) Crucial role for the Nalp3 inflammasome in the immunostimulatory properties of aluminium adjuvants. *Nature* 453:1122–1126.
13. Mariathasan S, et al. (2006) Cryopyrin activates the inflammasome in response to toxins and ATP. *Nature* 440:228–232.
14. Kanneganti TD, et al. (2006) Bacterial RNA and small antiviral compounds activate caspase-1 through cryopyrin/Nalp3. *Nature* 440:233–236.
15. Guarda G, et al. (2009) T cells dampen innate immune responses through inhibition of NLRP1 and NLRP3 inflammasomes. *Nature* 460:269–273.
16. Suzuki T, et al. (2007) Differential regulation of caspase-1 activation, pyroptosis, and autophagy via Ipaf and ASC in *Shigella*-infected macrophages. *PLoS Pathog* 3(8):e111.
17. Sutterwala FS, et al. (2007) Immune recognition of *Pseudomonas aeruginosa* mediated by the IPAF/NLRC4 inflammasome. *J Exp Med* 204:3235–3245.
18. Mariathasan S, et al. (2004) Differential activation of the inflammasome by caspase-1 adaptors ASC and Ipaf. *Nature* 430:213–218.
19. Miao EA, et al. (2010) Innate immune detection of the type III secretion apparatus through the NLRC4 inflammasome. *Proc Natl Acad Sci USA* 107:3076–3080.
20. Miao EA, et al. (2006) Cytoplasmic flagellin activates caspase-1 and secretion of interleukin 1beta via Ipaf. *Nat Immunol* 7:569–575.
21. Molofsky AB, et al. (2006) Cytosolic recognition of flagellin by mouse macrophages restricts *Legionella pneumophila* infection. *J Exp Med* 203:1093–1104.
22. Sutterwala FS, Flavell RA (2009) NLRC4/IPAF: A CARD carrying member of the NLR family. *Clin Immunol* 130:2–6.
23. Sadasivam S, et al. (2005) Caspase-1 activator Ipaf is a p53-inducible gene involved in apoptosis. *Oncogene* 24:627–636.
24. Thalappilly S, Sadasivam S, Radha V, Swarup G (2006) Involvement of caspase 1 and its activator Ipaf upstream of mitochondrial events in apoptosis. *FEBS J* 273:2766–2778.
25. Ghiringhelli F, et al. (2009) Activation of the NLRP3 inflammasome in dendritic cells induces IL-1beta-dependent adaptive immunity against tumors. *Nat Med* 15: 1170–1178.
26. Rakoff-Nahoum S, Medzhitov R (2007) Regulation of spontaneous intestinal tumorigenesis through the adaptor protein MyD88. *Science* 317:124–127.
27. Salcedo R, et al. (2010) MyD88-mediated signaling prevents development of adenocarcinomas of the colon: Role of interleukin 18. *J Exp Med* 207:1625–1636.
28. Allen IC, et al. (2010) The NLRP3 inflammasome functions as a negative regulator of tumorigenesis during colitis-associated cancer. *J Exp Med* 207:1045–1056.
29. Dupaul-Chicoine J, et al. (2010) Control of intestinal homeostasis, colitis, and colitis-associated colorectal cancer by the inflammatory caspases. *Immunity* 32:367–378.
30. Zaki MH, et al. (2010) The NLRP3 inflammasome protects against loss of epithelial integrity and mortality during experimental colitis. *Immunity* 32:379–391.
31. Bauer C, et al. (2010) Colitis induced in mice with dextran sulfate sodium (DSS) is mediated by the NLRP3 inflammasome. *Gut* 59:1192–1199.
32. Jarry A, et al. (1999) Interleukin 1 and interleukin 1beta converting enzyme (caspase 1) expression in the human colonic epithelial barrier. Caspase 1 downregulation in colon cancer. *Gut* 45:246–251.
33. Oviedo NJ, Beane WS (2009) Regeneration: The origin of cancer or a possible cure? *Semin Cell Dev Biol* 20:557–564.
34. Collado M, Blasco MA, Serrano M (2007) Cellular senescence in cancer and aging. *Cell* 130:223–233.
35. Uronis JM, et al. (2009) Modulation of the intestinal microbiota alters colitis-associated colorectal cancer susceptibility. *PLoS ONE* 4:e6026.
36. Becker C, Fantini MC, Neurath MF (2006) High resolution colonoscopy in live mice. *Nat Protoc* 1:2900–2904.
37. O'Connor W, Jr., et al. (2009) A protective function for interleukin 17A in T cell-mediated intestinal inflammation. *Nat Immunol* 10:603–609.

Supporting Information

Hu et al. 10.1073/pnas.1016814108

SI Materials and Methods

Endoscopic Procedures. Colonoscopy was performed at indicated time points to monitor for severity of colitis and tumorigenesis. According to the murine endoscopic index of colitis severity system (1), colitis was scored on five parameters: granularity of mucosal surface, stool consistence, vascular pattern, translucency of the colon, and fibrin visible (score between 0 and 3 for each parameter). Tumor sizes were graded from 1 to 5 as follows: Grade 1 (very small but detectable tumor), Grade 2 (tumor covering up to one-eighth of colonic circumference), Grade 3 (tumor covering up to one-fourth of the colonic circumference), Grade 4 (tumor covering up to half of the colonic circumference), and Grade 5 (tumor covering more than half of the colonic circumference) (1). Tumors observed during endoscopy were counted to obtain the total number of tumors per animal. The size of each tumor in every mouse was recorded, and the sum of all tumor sizes per mouse was calculated to be the tumor score.

Histopathology. After processing, colons were embedded lengthwise in paraffin (Blue RiBbon; Surgipath Medical Industries). Blocks were sectioned to the level of the lumen and then the next 5-μm section was stained with H&E, followed by placement of coverslips by routine methods. Colons were evaluated and were assigned scores by investigators blinded to experimental manipulation. Each section was evaluated for pathological changes in the mucosa, submucosa, muscularis externa, and serosa, including inflammation, edema, mucosal changes of ulceration, hyperplasia, and attenuation, with crypt loss or abscess noted by examination of H&E-stained slides assessed at low power and higher power and assigned scores for the presence and extent (overall severity) of the tissue changes by a semiquantitative criterion-based method (2). Severity scores ranged from 0 to 5 as follows: 0, within normal limits or absent; 1, minimal; 2, mild; 3, moderate; 4, marked; and 5, severe. Digital light microscopic images were recorded with a Zeiss Axio Imager.A1 microscope, AxioCam MRc5 camera, and AxioVision 4.7.1 imaging software (Carl Zeiss Microimaging).

Immunohistochemistry. Paraffin-embedded sections were dehydrated and incubated with the following antibodies: anti-BrdU (1:4,000; Sigma), anti-Ki67 (1:100, Thermo; Lab Vision), anti-CD3 (1:400, Biocare Medical), and anti-myeloperoxidase (MOP) (1:100, Thermo; Lab Vision), anti-Nk1.1 (1:100, Novus Biologicals). DAKO EnVision System was used for detection. All sections were counterstained with hematoxylin. For BrdU proliferation assay, mice were injected intraperitoneally with 1 mL BrdU (Sigma) solution, and killed 24 h after injection. TUNEL staining was performed using ApoAlert DNA Fragmentation Assay Kit (Clontech) and ApopTag Peroxidase In Situ Apoptosis Detection Kit (Millipore) according to the manufacturer's instructions. Percentage of TUNEL-positive cells in tumor tissues were counted on slides from five sections of each slide and divided by the total cell number of each field at the magnification 10×40. $Ki67^+$ cells were quantitated from 30 crypts of each mouse at day 15 of the colitis-associated colorectal cancer (CAC) model regimen. $BrdU^+$ cells were quantitated from $\geq$ 25 crypts of each mouse at day 15. The percentage of $Ki67^+$ and $BrdU^+$ cells in tumor tissues were counted from six sections of each slide and divided by the total cell number of each field at the magnification of 10×100. The $CD3^+$ and $MOP\text{-}1^+$ cells in tumor tissues were counted from greater than or equal to six fields of tumor tissue from each slide at the magnification of 10×100.

Isolation of Epithelial Cells and Hematopoietic Cells from the Intestine. Epithelial cells and hematopoietic cells were isolated from the freshly dissected colon. After removal of the Payer's patches and the adventitial fat, the colon was cut longitudinally and washed with PBS. For disruption of the epithelial cells, the colon was incubated in HBSS/EDTA in a 37 °C water bath, manually shaking for 20 min. The supernatant was collected and further separated in $CD45^+$ (IEL) and negative cells using MACS. The remaining colon was cut into small pieces and digested using Collagenase/DNase incubation in a 37 °C water bath, manually shaking, and afterward filtered through a 100-μm cell strainer. $CD45^+$ cells (LPL) were purified using MACS. In a second step $CD45^+$ IEL and LPL cells were further purified using a MoFlo cell sorter. The purity of $CD45^+$ cells was > 95%, epithelial cells were > 99% $CD45^-$.

TaqMan Gene Expression Assays' Catalog Numbers. Caspase-1: Mm00438023_m1; NLRC4: Mm01233150_m1; NLRP3: Mm00840904_m1; IL-17a: Mm00439618_m1; IFN-γ: Mm00801778_m1; IL-18: Mm00434225_m1; IL-11: Mm00434162_m1; IL-1β: Mm01336189_m1; TNF-α: Mm00443258_m1; IL-22: Mm00444241_m1; IL-6: Mm00446190_m1.

1. Becker C, Fantini MC, Neurath MF (2006) High resolution colonoscopy in live mice. *Nat Protoc* 1:2900–2904.

2. O'Connor W, Jr., et al. (2009) A protective function for interleukin 17A in T cell-mediated intestinal inflammation. *Nat Immunol* 10:603–609.

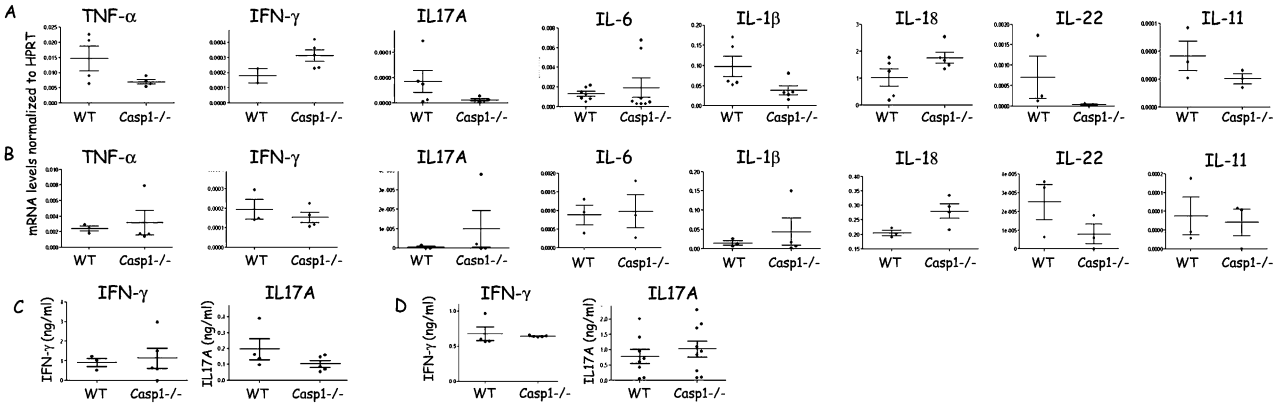

Fig. S1. Cytokine quantification in WT and Casp1$^{-/-}$ mice in the acute and chronic phases of colitis. TNF-α, IFN-γ, IL-1β, IL-18, IL-6, IL-22, IL-11, and IL-17A mRNA expression in WT and Casp1$^{-/-}$ colons was measured at day 15 of the CAC regimen (*A*) or 10 d following the cessation of the last cycle of dextran sodium sulfate (DSS) treatment (*B*). For protein measurement, 1-cm halved colon explants were incubated for 24 h and ELISA was performed on the supernatant during acute and chronic phases of colitis (*C* and *D*, respectively).

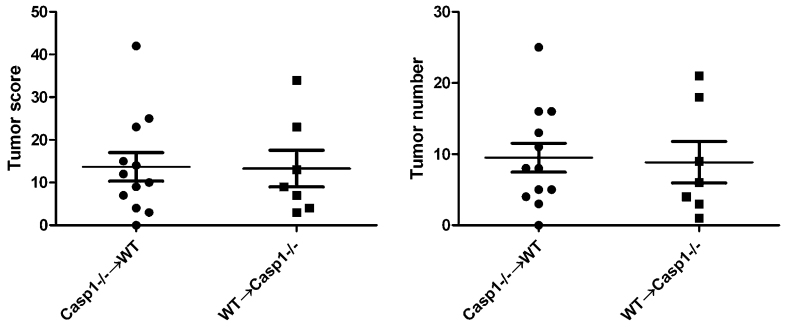

Fig. S2. Bone-marrow chimera experiments. WT or Casp1$^{-/-}$ bone marrow was transferred to WT or Casp1$^{-/-}$ mice following sublethal irradiation (two doses of 550 rad). Azoxymethane (AOM)-DSS CAC regimen was induced 8 wk later. Tumor load and tumor numbers/mouse were determined by colonoscopy on day 65 of the CAC regimen.

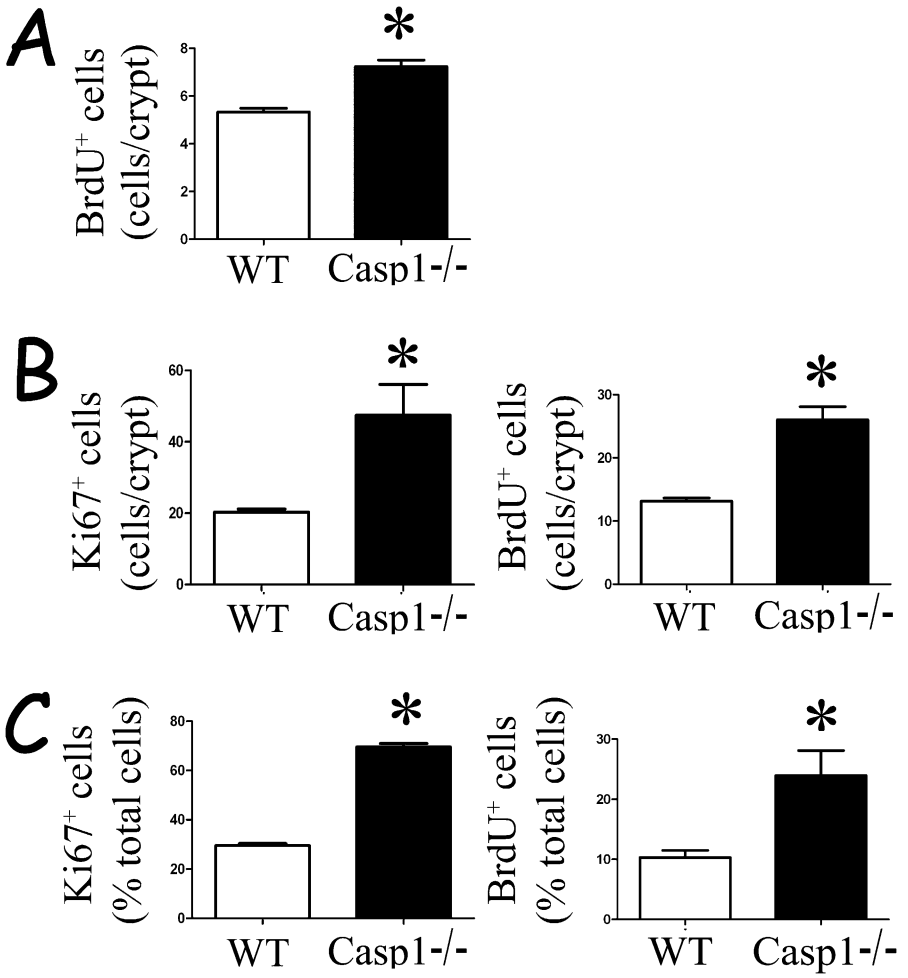

Fig. S3. Enhanced colon epithelial cell proliferation during the acute inflammatory phase and tumor cell proliferation in Casp1$^{-/-}$ mice. BrdU^{+} cells were quantitated from 30 crypts of each mouse at baseline (*A*) and day 15 of the CAC regimen (*B*, *Left*). BrdU^{+} cells were quantitated from ≥ 25 crypts of each mouse at day 15 of the CAC regimen (*B*, *Right*). The percentage of Ki67^{+} and BrdU^{+} cells (*C*) in tumor tissues were counted from six sections of each slide and divided by the total cell number of each field at the magnification 10 × 100. *P* values < 0.05 were considered statistically significant.

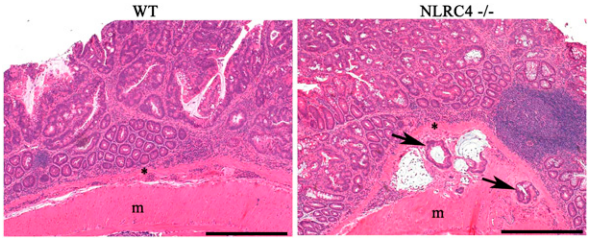

Fig. S4. NLRC4$^{-/-}$ mice develop aggressive locally invasive tumors. Representative histopathologic sections of colon adenocarcinomas and foci of tumor invasion from WT and NLRC4$^{-/-}$ mice. Invasive tumor foci (arrows) were not found in WT mice, but they were present in 66% of NLRC4$^{-/-}$ mice, where tumor foci were surrounded by abundant amounts of pale blue mucin. H&E staining; *muscularis mucosae; m, mascularis externa. (Scale bars, 200 μm.)

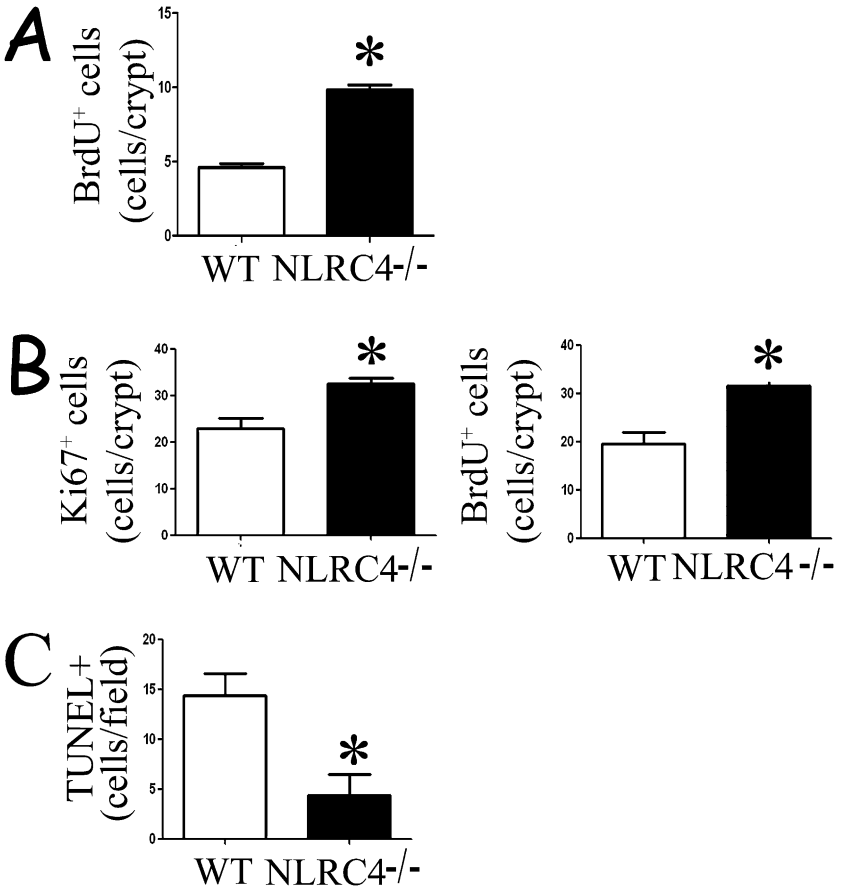

Fig. S5. Enhanced colon epithelial cell proliferation during the acute inflammatory phase and tumor cell proliferation in NLRC4$^{-/-}$ mice. BrdU^{+} cells were quantified from ≥ 25 crypts of each mouse at steady-state conditions (*A*); Ki67^{+} and BrdU^{+} cells were quantitated from ≥ 25 crypts of each mouse at day 15 of the CAC regimen (*B*). TUNEL-positive cells in tumor tissues were counted from greater than or equal to six fields of each slide at the magnification 10 × 40 (*C*). *P* values < 0.05 were considered statistically significant.